Continuous Monitoring and Analysis of Pandanus Amaryllifolius Microbial Fuel Cell Power Generation in Daily Solar Radiation

Teng Howe Cheng[1], Kok Boon Ching[2], Chessda Uttraphan[3],Yee Mei Heong[4]
[1,2,3,4]*Department of Engineering Education, Faculty of Technic and Vocational Education,,*
Universiti Tun Hussein Onn Malaysia, Parit Raja, 86400 Batu Pahat, Johor, Malaysia.

Abstract- Conventional power generation usually releases pollutants, which cause damages to the environment and are harmful to human health. This leads to the growing development of renewable energies, which greatly reduces contamination. Plant microbial fuel cell (P-MFC) is an innovative technology which is inexpensive, does not pollute the environment and provides flexibility to produce energy anywhere. Nevertheless, the system is still at the initial stage for the commercialization purpose and has low and inconsistent power output. In the current research, the monitoring and analysis of Pandanus Amaryllifolius as the main substrate of microbial fuel cell were conducted and compared with the traditional MFC. Important parameters such as electrode area contact, light intensity, temperature, humidity and soil pH were monitored in an open environment for five consecutive days to investigate the electrical energy conversion process via electrochemically active bacteria inside the soil. It was observed that the power output increases in accordance with temperature, light intensity and terminal size, satisfying the Nernst potential equation. Conversely, the soil pH does not seem to have a significant effect on the P-MFC power generation.
Keywords – Plant microbial fuel cell, Bioenergy, Waste energy harvesting, Rhizodeposits, Green energy

I. INTRODUCTION

The demand for clean energy has grown progressively year by year, shifting from the conventional fossil fuel energy to renewable energy technologies. This transition brings a few key advantages: sustainable energy production, lower operating cost and low-carbon emission process while reducing greenhouse gases (GHGs) [1]–[4]. Since the development of existing renewable energy technology such as solar and hydropower is already at its peak, scientists have shifted their interest from weather-dependent renewable energy to weather-independent electricity production system. In 2008, Strik et al. [5] proposed plant microbial fuel cells (P-MFC) that harvest energy from electrochemically active bacteria (EAB), which synthesizes organic compounds released by the plant roots into the rhizosphere. This electricity production system can potentially generate 5800 kWh ha-1 year-1.

P-MFC possess major advantages as compared to other renewable energy technologies as it can generate sustainable energy without much conflict and it also can be operated anywhere with no geographical barriers [6], [7]. Theoretically, P-MFC utilizes the microbes in the rhizosphere, where the oxidation of the organic compound takes place [8]–[10]. The P-MFC process starts with the deposition of an organic compound from the plant roots during photosynthesis, which is then consumed by microbes that liberate electrons before transferring the electrons from the anode to the cathode, which is optionally separated by membranes.

Despite being able to generate electricity without harming the environment, P-MFC is often hindered by its own problem, which is the fact that P-MFC has small energy output. Therefore, many studies have been conducted to revamp the electricity generation under controlled conditions [11]–[16]. However, the system performance is still very reliant on several aspects such as the electrode materials and the plant and soil types, which influence the compatibility of the microbial community adherence. The aim of this paper to focus on the monitoring and analysis of influential variables on electricity generation of P-MFC, such as electrode area contact, temperature, light intensity and pH of the soil.

II. MATERIALS AND METHODS

The assessment first requires the setting up of P-MFC, using Pandanus Amaryllifolius as the main source of substrate for the microbes. Two P-MFCs, which are P-MFC A and P-MFC B, with another two MFCs without plant will be monitored to determine the parameters that will significantly affect the amount of power generation. The overall process is shown in Figure 1.

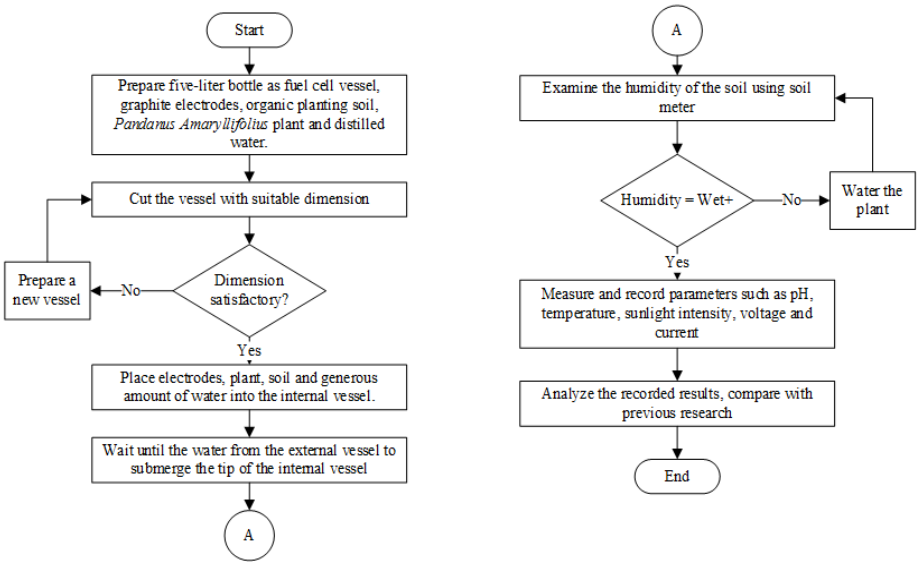

Figure 1. Flowchart for the overall experimental process

2.1 Construction of P-MFC

The fuel cell chamber is constructed using plastic bottles with a capacity of five liters. The dimensions of the external vessel are 20.5 cm in height and 15.5 cm in length and width. The internal vessel that holds the soil is dimensioned at 10 cm in height and 15.5 cm in length and width. The inverse-pyramid-shaped internal vessel can hold up to a total volume of 1600 cm3 of soil, where the bottle cap at the bottom tip is perforated to enable the flow of excessive water. The overall fuel cell chamber concept is described in Figure 2.

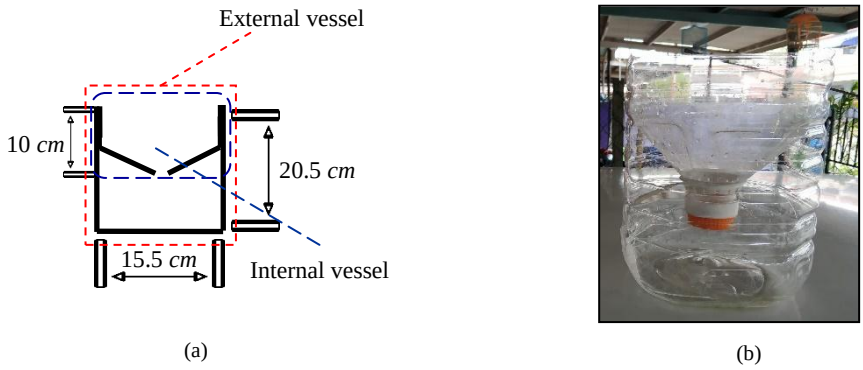

Figure 2. Structure of the fuel cell chamber for P-MFC: (a) Dimensions of the vessel and (b) a simple vessel

Four graphite electrodes with a length of 10 cm and diameter of 1 cm are prepared as the anodes and cathodes of the P-MFC. Each electrode is then tied by a 0.6mm single-core copper wire to lengthen the possible measurement distance. The graphite electrodes for the cathodes are then wrapped inside a cellulose membrane tube in order to distinguish it from the anode, as depicted in Figure 3.

Figure 3 Preparation of graphite electrodes for the P-MFC. The cathodes are wrapped in a cellulose membrane and the anodes are without a membrane.

Organic planting soil that includes coco peat, burnt soil, river sand, burnt husk, rich humus and charcoal powder is used as the base of the P-MFC. The anode electrode is then placed under the roots of the Pandanus Amaryllifolius plant before it is covered with the soil. Subsequently, the cathode electrode is embedded inside the soil with different depths, i.e., 5 cm for P-MFC A and fully implanted at 10 cm for P-MFC B. Distilled water is then poured into the vessels until it drips from the bottom tip of the internal vessel, as illustrated in Figure 4, to retain the soil moisture thoroughly.

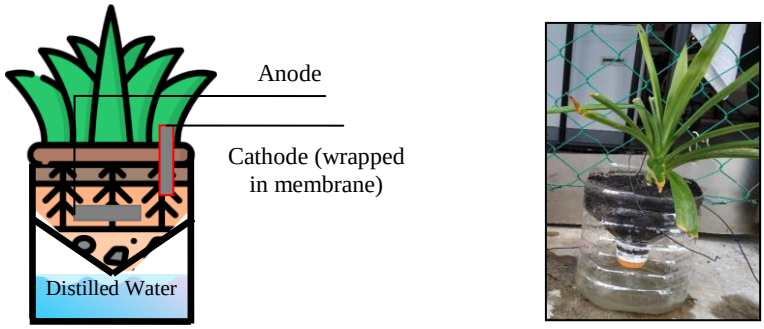

Figure 4. Plant microbial fuel cell vessel constructed by placing the anode under the root and placing the cathode wrapped in membrane exposed to the air. (a) Illustration of P-MFC with labels and (b) the P-MFC set-up.

2.2 Monitoring the constructed P-MFC

Both P-MFCs and MFCs are then placed outdoor for five days to ensure normal daily sunlight exposure as to promote plant photosynthesis and bacteria growth. The soil of the vessel is watered regularly to retain the dampness, as humidity is one of the important aspects that keep the electron flow efficiently. Other parameters such as voltage, current, temperature, light intensity and pH are taken periodically using Victor VC830L digital multimeter and AMTAST AMT-300 soil meter once every three hours.

The soil is tested for acetate at the start and the end of the experiment, where the 16 g of soil harvested is flushed with N2 three times to establish an anaerobic condition and added with 250 ml of sterile anaerobic mineral solution containing NaHCO3, KH2PO4, MgCl2.6H2O, NaCl, NH4Cl, CaCl2.2H2O, cysteine and HCl.H2O. The soil sample is then shaken thoroughly by a shaker for two hours. The presence of aliphatic acids and monomeric aromatic compounds in the soil suspensions are determined by high-performance liquid chromatography (HLPC).

Upon completion of the experimentation process for five consecutive days, the recorded power generation value is plotted with a variable parameter which behaves linearly. The parameters affecting power generation can be determined significantly through the whole observation process. Statistical analysis is also made to compare the voltage and current generation at the start and the end of the experiment.

2.3 Bacterial RNA isolation and treatment

In order to determine the bacterial type which reacts with the electrodes, foreign deposits on the anode, which is suspected to be G. sulfurreducens biofilm, are scrapped and the RNA is extracted using the techniques referred [17].

The extracted RNA is treated to remove DNA contamination using the RNase-Free DNase I (Promega™) according to the manufacturer's suggested procedure and is verified for genomic DNA contamination by polymerase chain reaction (PCR) for 40 cycles (94˚C 120 sec; 94˚C 15 sec, 56˚C 60 sec, 72˚C 90 sec) using primers specific to G. sulfurreducens.
The RNA is then washed two times with 250 µl RNA Wash Solution (with ethanol added) and centrifuged at 12,000 × g for two minutes. To prevent DNA contamination, DNase Stop Solution is added and centrifuged at 12,000 × g for one minute and washed two times with RNA Wash Solution. The RNA is then ethanol-precipitated with 70% ethanol and resuspended in 100 µl of nuclease-free water, centrifuged at 12,000 × g for one minute, and the purified RNA is stored in an elution tube at −70˚C.

2.4 Biofilm identification
Among the important factors for the electron transfer from the anode terminal to the cathode terminal is the biofilm deposit on the surface of the anode. Hence, the excess biofilm sample scrapped from the anode terminal, which is dielectric, will be treated with a platinum coating of 2nm thickness before being placed for the field-emission scanning electron microscopy (FESEM). This process is conducted to avoid the charging effect that will cause the distortion of the SEM images.

2.5 Statistical analysis method
A normality test of open-circuit voltages (OCVs) is conducted with the Anderson-Darling test. However, a normalized result is not expected as bacteria grow in an exponential trend. Then, a Mann-Whitney test is performed to establish the differences between the cells' performance (P-MFC A, P-MFC B, MFC C and MFC D). Both tests use the SPSS Statistics program. Cell OCVs for the different periods are summarized in Table 1 with their means and standard deviations.

III. RESULTS AND DISCUSSION

This section discusses the results obtained from the experiment, which includes the effects of the different parameters involved and bacteria identification. Results taken from the four MFC are plotted on a graph. This part assesses the performances of both P-MFCs and MFCs, which differ in the cathode's area of contact.

3.1 Effects of electrode area, pH, light intensity and temperature on MFC and P-MFC
Open-circuit voltage (OCV), open-circuit current (I), average temperature, average light intensity and average soil pH are taken every three hours for each MFC. Power (P) is first calculated using Equation (1) and the average recorded results are given in Table 1.

$$P = V \times I \tag{1}$$

where V is voltage and I represent current. The calculated and recorded values are then plotted against time, as illustrated in Figure 5.

Table -1 Recorded ALI (Average Light Intensity), AT (Average Temperature), ApH (Average PH), OCV, OCI and Power for P-MFC and MFC

MFC Type	ALI (Lux)	AT (˚C)	ApH	OCV (mV)	OCI (µA)	Power (nW)
P-MFC A	6125.25±2322.35 (day), 63.15±12.70 (night)	27.5±4.5	3.93±0.55	80.23±40.8	63.19±33.55	6395.65±4207.55
P-MFC B			3.95±0.59	160.08±67.66	137.01±59.2	25808.53±13245.49
MFC C			4.31±0.67	18.05±16.55	10.94±10.25	356.5±453.98
MFC D			4.5±0.65	28.12±31.09	17.2±16.55	981.94±892.62

*(Mean)±(Std. Deviation)

Figure 5. Voltage vs. Time between P-MFC and MFC. It can be seen the (a) voltage, (b) current and (c) power spikes during mid-day as (d) temperature rises.

The Anderson-Darling test of normality is done with p-value of < 0.05 for all MFCs as expected. By comparing the variance parameters between P-MFC A and P-MFC B, it can be observed that the area of the electrode gives distinctive impacts on the power generation of P-MFC. The larger electrode area embedded in Plant B (8.639 cm2) channels more electron flow than the half-embedded electrode in Plant A (4.712 cm2), thus increasing the electrical generation density approximately by 275%. The upsurge of light intensity and temperature also contribute to the rise of power generation. Apparently, the soil pH is being acidified over time, but there is no significant influence on voltage generation.

3.2 Soil carbon compound content in anode chamber

In contrast to the concentration of acetate, the concentrations of other carboxylic acids detected are low.

Acetate is the only stable end product; the other products are subject to fluctuation between the values reported and

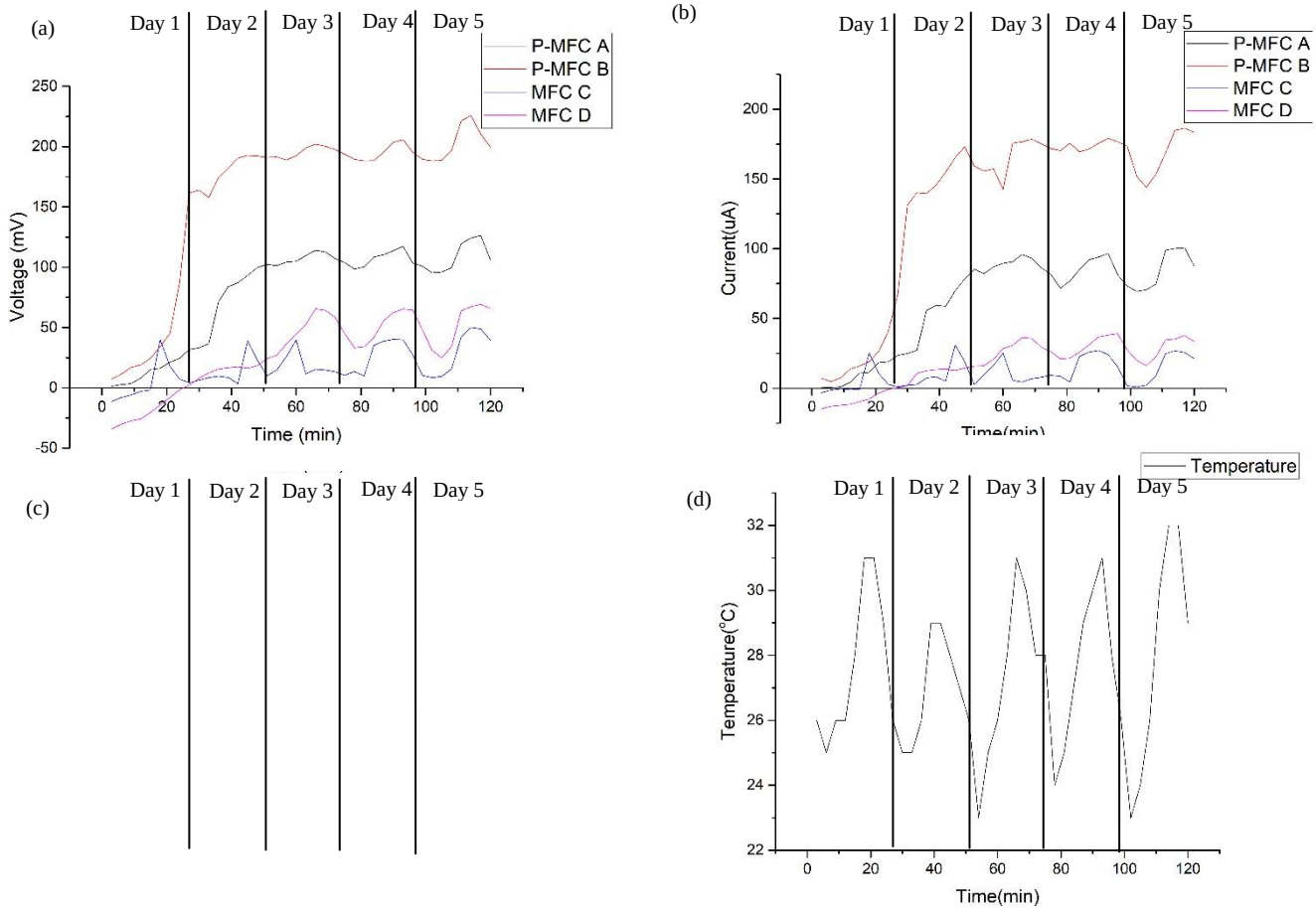

the nondetectable levels (Figure 6). Periodically, a few unidentified peaks are detected by HPLC on the basis of their levels of absorptivity. Their concentrations appear insignificant compared with that of acetate

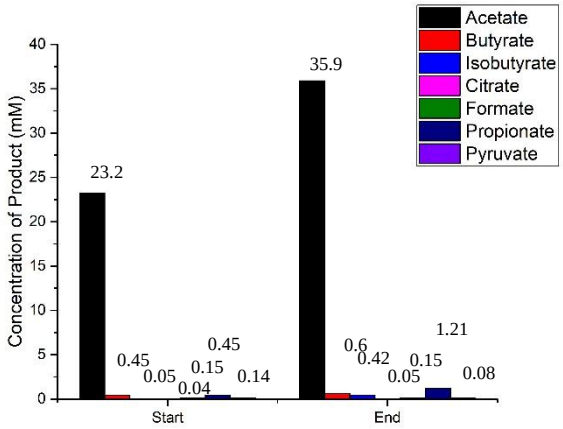

Figure 6. Concentration of organic C compound in soil at start and end of the monitoring process

3.3 Voltage versus time, temperature and power in MFCs

In the previous subsection, the plotted results reveal the effects of the changes in variables. The voltage generated by P-MFC increases with temperature.

In Day 1, all MFCs experience a lagging phase, hence the voltage generation is substantially low. It can be seen that the power generated in P-MFC B is exponentially increased at the end of Day 1. The power levels for both P-MFCs start to stabilize in the following day and enter a stationary phase in Days 3, 4 and 5, while from the plant-less MFCs stabilize in Day 3 and consequently enter a stationary phase in the following days. From the graph, surges of power are observed during the peak temperature period of each day. By picking the maximum output from the graph, P-MFC B is able to generate 42 nW of power per 240.25 cm2 area, translating to power density up to 1.75 µWm-2 or 1.75 mWha-1.

In the Mann-Whitney test, P-MFC A and P-MFC B show a statistically significant difference in power generation with respect to other cells, indicating that the generation of power in cells with plants turn out to be similar in at least two reactors. However, the MFC C cell is similar to MFC D (Figure 7).

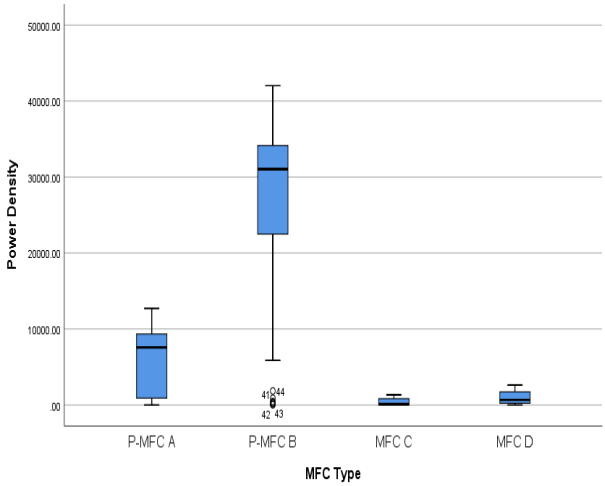

Figure 7. Comparison of power density generated by P-MFC and traditional MFC using the Mann-Whitney test

3.4 Bacteria identification on anode terminal

The physiological characteristics and phylogeny of strain PCA suggest a relationship to both Geobacter species and Desulfuromonas species and are confirmed by the maximum likelihood method [18]–[20]. The microscopic view of these proteobacteria is shown in Figure 8.

Both organisms are members of the delta proteobacteria [21], [22] and are obligately anaerobic, gram-negative rods which contain c-type cytochromes and the reduction of Fe(III).

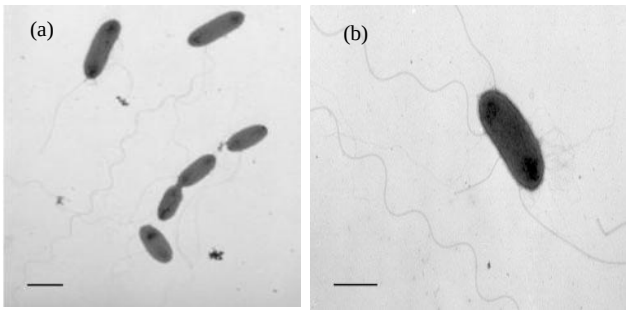

Figure 8. Microscopic view of negatively stained proteobacteria cells harvested from the anode, with the bar indicating 1 µm: (a) Community of proteobacteria and (b) visible flagella seen around the cell

3.5 Biofilm formation on anode terminal

During day time, plants perform photosynthesis under the sunlight. The photosynthesis process produces the necessary nutrients for the plant, and the excessive organic substrates will be excreted from the roots, called rhizodeposits, and will be consumed by the microorganisms living in the rhizosphere [6], [23]–[25]. Therefore, the plant microbial fuel cell is developed based on this concept.

By placing an anode electrode with less oxygen-obtainability inside the soil, the accumulation of EAB on the surface of the anode is forcedly formed and thus electrons are released during the redox reaction of the microbes on organic matters [26]–[28]. The electrons are then channeled through an external circuit, which will then be collected by the cathode. Due to the dependencies on the anode, EAB such as G. sulfurreducens excrete specialized proteins on the surface of the anode to form a conductive biofilm [29]–[33] which acts as an electron acceptor. These biofilms can be observed by the naked eye [34] and by using field-emission scanning electron microscopy (FESEM), as shown in Figure 9, which are then compared with other previous research [35], [36].

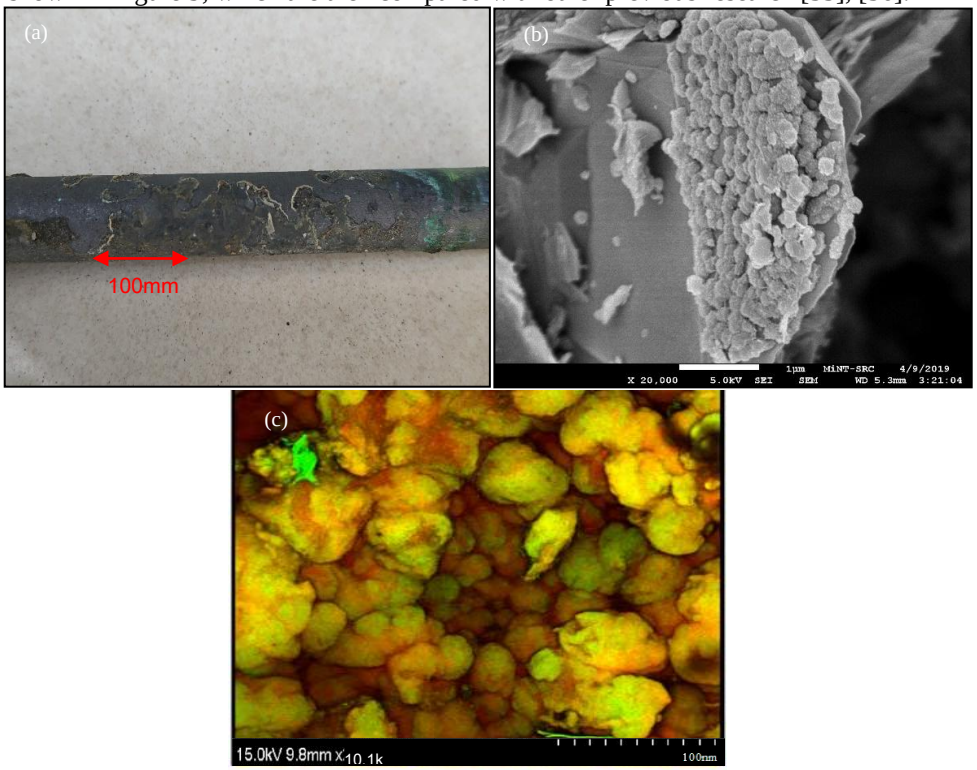

Figure 9. (a) Formation of biofilm seen on the surface of anode, (b) FESEM images of biofilm on the surface of anode and (c) Wild-type G. Sulfurreducens 3D-top-view [35]

3.5 Electrochemical reaction between acetate and bacteria

The exudation of organic C compounds by plants comprises a wide variety of simple and complex sugar such as amino acids, organic acids, phenolics [37], alcohols, polypeptides and proteins, hormones and enzymes. For instance, acetate (CH3COO-) is released through the exudation of plants. Through anodic oxidation in P-MFC, EAB will convert it to bicarbonate (HCO3) and hydrogen atom (H+), as shown in Equation (2).

$$CH_3COO^- + 4H_2O \xrightarrow[EAB]{} 2HCO_3^- + 9H^+ + 8e^- \quad (2)$$

Bicarbonate is a weak acid, hence this reaction explains the acidifying pH of the soil mentioned previously. The released electrons are then passed through the external circuit and collected by the cathode, while hydrogen atom penetrates the membranes of the cathode in order to form water with oxygen (O2) from the surroundings, as explained in Equation (3).

$$O_2 + 4H^+ + 4e^- \rightarrow 2H_2O \quad (3)$$

Referring to the cathodic reaction, small water droplets can be observed forming on the surface of the cathode, as shown in Figure 10.

Figure 10. Water droplets forming on the surface of cathode due to the recombination of hydrogen atom with oxygen from the air

The voltage generated from the P-MFC can be determined by the Nernst potential, as given in Equation (4):

$$E_{cell} = E^0_{cell} - \frac{RT}{nF}\ln Q_r \quad (4)$$

where Ecell is the cell potential (V), E0cell is the standard cell potential (V), R represents the universal gas constant (8.314 J mol-1 K-1), T represents temperature (K), n represents the number of electrons involved in the reaction, F represents the Faraday's constant (9.65×104 C mol-1) and Q represents the reaction quotient during the P-MFC operation.

By combining Equations (2) and (4), the anodic reaction can be observed:

$$E_{an} = E^0_{an} - \frac{RT}{8F}\ln\left(\frac{\left[CH_3COO^-\right]}{\left[HCO_3\right]^2\left[H^+\right]^9}\right) \quad (5)$$

Where Ean is the anode potential (V) and E0an is the standard anode potential (V). Since the concentration and composition of the organic substrate in P-MFC are mainly unknown, the precise Nernst potential of the anode is hard to be determined. Hence, the standard open-cell potential of the anode, E^0_{an}, is used, which is typically −0.289 V vs. the standard hydrogen electrode. The cathodic reaction can be rewritten as:

$$E_{cath} = E^0_{cath} - \frac{RT}{4F}\ln\left(\frac{1}{pO_2\left[H^+\right]^4}\right) \quad (6)$$

Where Ecath is the cathode potential (V) and E0cath is the standard cathode potential (V). The standard cathode potential with oxygen reduction is typically +0.805 V vs. the standard hydrogen electrode. Ideally, the maximum voltage generated by P-MFC of 1.1 V can be attained with oxygen reduction on the cathode:

$$E_{cell} = E_{cath} - E_{an} \quad (7)$$

However, the maximum voltage cannot be obtained due to non-ideal situations such as internal resistance of P-MFC, loss of electrons to the surroundings and activation potential loss.

IV. CONCLUSION

The assessment concludes that the electrode's exposed area, light intensity and temperature can affect the power output of P-MFC. High light intensity provides sunlight for plant photosynthesis, which provides a substrate for the microbes [38]–[40], while higher temperature can lead to higher metabolism of G. Sulfurreducens. On the other hand, soil pH does not seem to have any effect but may have consequences on the plant's health. In the same working conditions, both P-MFC A and P-MFC B perform in a similar pattern, where the higher the temperature, the higher is the power output. Eventually, the output from P-MFC B fits the model of the bacterial growth curve by Zwietering et al. [41]. Nevertheless, the power outputs from the P-MFCs are still not satisfactory enough to power electronic applications. The optimization on the operation of P-MFC can be improved by utilizing biocompatible electrodes that do not corrode, while increasing the surface area of the anode and cathode and maintaining the optimum temperature for the microbes.

V. ACKNOWLEDGEMENTS

The author gratefully acknowledges financial support from the Research Management Centre, UTHM under Grant (U957) and Research Fund (E15501).

VI. ABBREVIATIONS

Table -2 Nomenclature

Section	Symbol/ Abbreviations	Explanation
I	GHGs	Greenhouse Gases
	P-MFC	Plant Microbial Fuel Cell
	EAB	Electrochemically Active Bacteria
II	RNA	Ribonucleic Acid
	DNA	Deoxyribonucleic acid
	PCR	Polymerase Chain Reaction
	FESEM	Field Emission Scanning Electron Microscopy
	N2	Nitrogen
	NaHCO3	Sodium Hydrogen Carbonate
	KH2PO4	Potassium dihydrogen phosphate
	MgCl2	Magnesium chloride hexahydrate
	NaCl	Sodium Chloride
	NH4Cl	Ammonium Chloride
	CaCl2.2H2O	Calcium Chloride Dihydrate
	HCl:	Hydrogen Chloride
	HPLC	High-performance liquid chromatography
III	E_{an}	Anode Nernst potential (V)
	E_{an}^{0}	Standard anode potential (V)
	E_{cath}	Cathode Nernst potential (V)
	E_{cath}^{0}	Standard cathode potential (V)
	E_{cell}	Cell potential (V)
	E_{cell}^{0}	Standard cell potential (V)
	F	Faraday's constant ($9.65\times10^{4}\,\mathrm{C\,mol^{-1}}$)
	n	Number of electrons involved in reaction
	Q_r	Reaction quotient of the P-MFC reaction
	R	Universal gas constant ($8.314\,\mathrm{J\,mol^{-1}\,K^{-1}}$)
	T	Temperature (K)

	CH_3COO^-	Acetate
	H^+	Hydrogen atom
	H_2O	Water
	HCO_3^-	Bicarbonate
	pO_2	Partial oxygen pressure (^{Pa})

VII. REFERENCES

[1] H. C. Teng, B. C. Kok, C. Uttraphan, and M. H. Yee, "A Review on Energy Harvesting Potential from Living Plants : Future Energy Resource," Int. J. Renew. Energy Res., vol. 8, no. 4, pp. 2598–2614, 2018.

[2] A. Louwen, W. G. J. H. M. Van Sark, A. P. C. Faaij, and R. E. I. Schropp, "Re-assessment of net energy production and greenhouse gas emissions avoidance after 40 years of photovoltaics development," Nat. Commun., vol. 7, pp. 1–9, 2016.

[3] T. Tsoutsos, N. Frantzeskaki, and V. Gekas, "Environmental impacts from the solar energy technologies," Energy Policy, vol. 33, no. 3, pp. 289–296, 2005.

[4] J. B. A. Arends et al., "Greenhouse gas emissions from rice microcosms amended with a plant microbial fuel cell," Appl. Microbiol. Biotechnol., vol. 98, no. 7, pp. 3205–3217, 2014.

[5] D. P. B. T. B. Strik, H. V. M. H. (Bert), J. F. H. Snel, and C. J. N. Buisman, "Green electricity production with living plants and bacteria in a fuel cell," Int. J. Energy Res., vol. 33, no. 4, pp. 23–40, 2008.

[6] R. Nitisoravut and R. Regmi, "Plant microbial fuel cells: A promising biosystems engineering," Renew. Sustain. Energy Rev., vol. 76, no. September 2016, pp. 81–89, 2017.

[7] O. Kaplan, U. Yavanoglu, and F. Issi, "Country study on renewable energy sources in Turkey," 2012 Int. Conf. Renew. Energy Res. Appl. ICRERA 2012, pp. 1–5, 2012.

[8] Y. Y. Choo et al., "A Method to Harvest Electrical Energy from Living Plants," J. Sci. Technol., vol. 5, no. 1, pp. 79–90, 2013.

[9] P.-F. Tee, M. O. Abdullah, I. A. W. Tan, M. A. M. Amin, C. Nolasco-Hipolito, and K. Bujang, "Effects of temperature on wastewater treatment in an affordable microbial fuel cell-adsorption hybrid system," J. Environ. Chem. Eng., vol. 5, no. 1, pp. 178–188, Feb. 2017.

[10] R. A. Timmers, D. P. B. T. B. Strik, H. V. M. Hamelers, and C. J. N. Buisman, "Electricity generation by a novel design tubular plant microbial fuel cell," Biomass and Bioenergy, vol. 51, pp. 60–67, 2013.

[11] J. R. Kim, S. Cheng, S.-E. Oh, and B. E. Logan, "Power Generation Using Different Cation, Anion, and Ultrafiltration Membranes in Microbial Fuel Cells," Environ. Sci. Technol., vol. 41, no. 3, pp. 1004–1009, 2007.

[12] Y. Zhang et al., "A graphene modified anode to improve the performance of microbial fuel cells," J. Power Sources, vol. 196, no. 13, pp. 5402–5407, 2011.

[13] B. Min, Ó. B. Román, and I. Angelidaki, "Importance of temperature and anodic medium composition on microbial fuel cell (MFC) performance," Biotechnol. Lett., vol. 30, no. 7, pp. 1213–1218, 2008.

[14] A. Larrosa-Guerrero, K. Scott, I. M. Head, F. Mateo, A. Ginesta, and C. Godinez, "Effect of temperature on the performance of microbial fuel cells," Fuel, vol. 89, no. 12, pp. 3985–3994, 2010.

[15] Y. Ye, X. Zhu, and B. E. Logan, "Effect of buffer charge on performance of air-cathodes used in microbial fuel cells," Electrochim. Acta, vol. 194, pp. 441–447, Mar. 2016.

[16] M. Rahimnejad, T. Jafary, F. Haghparast, G. D. Najafpour, and A. A. Ghoreyshi, "Nafion as a nanoproton conductor in microbial fuel cells," Turkish J. Eng. Environ. Sci., vol. 34, no. 4, pp. 289–291, 2010.

[17] D. E. Holmes et al., "Microarray and genetic analysis of electron transfer to electrodes in Geobacter sulfurreducens," vol. 8, pp. 1805–1815, 2006.

[18] S. Guindon, J. F. Dufayard, V. Lefort, M. Anisimova, W. Hordijk, and O. Gascuel, "New algorithms and methods to estimate maximum-likelihood phylogenies: Assessing the performance of PhyML 3.0," Syst. Biol., vol. 59, no. 3, pp. 307–321, 2010.

[19] J. Drury, J. Clavel, M. Manceau, and H. Morlon, "Estimating the effect of competition on trait evolution using maximum likelihood inference," Syst. Biol., vol. 65, no. 4, pp. 700–710, 2016.

[20] D. E. Holmes, K. P. Nevin, and D. R. Lovley, "Comparison of 16S rRNA, nifD, recA, gyrB, rpoB and fusA genes within the family Geobacteraceae fam. nov," Int. J. Syst. Evol. Microbiol., vol. 54, no. 5, pp. 1591–1599, 2004.

[21] N. R. Shin, T. W. Whon, and J. W. Bae, "Proteobacteria: Microbial signature of dysbiosis in gut microbiota," Trends Biotechnol., vol. 33, no. 9, pp. 496–503, 2015.

[22] Y. Wang, W. Lin, and Y. Pana, "High diversity of magnetotactic Deltaproteobacteria in a freshwater Niche," Appl. Environ. Microbiol., vol. 79, no. 8, pp. 2813–2817, 2013.

[23] J. Pausch and Y. Kuzyakov, "Carbon input by roots into the soil: Quantification of rhizodeposition from root to ecosystem scale," Glob. Chang. Biol., vol. 24, no. 1, pp. 1–12, 2018.

[24] L. Mwafulirwa et al., "Barley genotype influences stabilization of rhizodeposition-derived C and soil organic matter mineralization," Soil Biol. Biochem., vol. 95, pp. 60–69, 2016.

[25] D. L. Jones, A. Hodge, and Y. Kuzyakov, "Plant and mycorrhizal regulation of rhizodeposition," New Phytol., vol. 163, no. 3, pp. 459–480, 2004.

[26] V. F. Passos, S. Aquino Neto, A. R. de Andrade, and V. Reginatto, "Energy generation in a Microbial Fuel Cell using anaerobic sludge from a wastewater treatment plant," Sci. Agric., vol. 73, no. 5, pp. 424–428, 2016.

[27] S. Venkata Mohan, G. Velvizhi, J. Annie Modestra, and S. Srikanth, "Microbial fuel cell: Critical factors regulating bio-catalyzed electrochemical process and recent advancements," Renew. Sustain. Energy Rev., vol. 40, pp. 779–797, Dec. 2014.

[28] R. A. Timmers et al., "Microbial community structure elucidates performance of glyceria maxima plant microbial fuel cell," Appl. Microbiol. Biotechnol., vol. 94, no. 2, pp. 537–548, 2012.

[29] J. M. Sonawane, A. Yadav, P. C. Ghosh, and S. B. Adeloju, "Recent advances in the development and utilization of modern anode materials for high performance microbial fuel cells," Biosens. Bioelectron., vol. 90, no. September 2016, pp. 558–576, 2017.

[30] M. M. Mardanpour, S. Yaghmaei, and M. Kalantar, "Modeling of microfluidic microbial fuel cells using quantitative bacterial transport parameters," J. Power Sources, vol. 342, pp. 1017–1031, 2017.

[31] K. Schneider, R. J. Thorne, and P. J. Cameron, "An investigation of anode and cathode materials in photomicrobial fuel cells," Philos. Trans. R. Soc. A Math. Phys. Eng. Sci., vol. 374, no. 2061, 2016.
[32] A. Mehdinia, E. Ziaei, and A. Jabbari, "Facile microwave-assisted synthesized reduced graphene oxide/tin oxide nanocomposite and using as anode material of microbial fuel cell to improve power generation," Int. J. Hydrogen Energy, vol. 39, no. 20, pp. 10724–10730, 2014.
[33] C. Santoro, C. Arbizzani, B. Erable, and I. Ieropoulos, "Microbial fuel cells: From fundamentals to applications. A review," J. Power Sources, vol. 356, pp. 225–244, 2017.
[34] J. H. Moreno Osorio, G. Pinto, A. Pollio, L. Frunzo, P. N. L. Lens, and G. Esposito, "Start-up of a nutrient removal system using Scenedesmus vacuolatus and Chlorella vulgaris biofilms," Bioresour. Bioprocess., vol. 6, no. 1, p. 27, 2019.
[35] K. P. Nevin et al., "Anode biofilm transcriptomics reveals outer surface components essential for high density current production in Geobacter sulfurreducens fuel cells," PLoS One, vol. 4, no. 5, 2009.
[36] A. Benítez-Cabello et al., "RT-PCR-DGGE analysis to elucidate the dominant bacterial species of industrial Spanish-style green table olive fermentations," Front. Microbiol., vol. 7, no. AUG, pp. 1–11, 2016.
[37] G. Neumann and E. Martinoia, "Cluster roots - An underground adaptation for survival in extreme environments," Trends Plant Sci., vol. 7, no. 4, pp. 162–167, 2002.
[38] M. Rahimnejad, A. Adhami, S. Darvari, A. Zirepour, and S. E. Oh, "Microbial fuel cell as new technol ogy for bioelectricity generation: A review," Alexandria Eng. J., vol. 54, no. 3, pp. 745–756, 2015.
[39] M. Esfandyari, M. A. Fanaei, R. Gheshlaghi, and M. Akhavan Mahdavi, "Mathematical modeling of two-chamber batch microbial fuel cell with pure culture of Shewanella," Chem. Eng. Res. Des., vol. 117, pp. 34–42, 2017.
[40] Y.-Q. Wang, H.-X. Huang, B. Li, and W.-S. Li, "Novelly developed three-dimensional carbon scaffold anodes from polyacrylonitrile for microbial fuel cells," J. Mater. Chem. A, vol. 3, no. 9, pp. 5110–5118, 2015.
[41] M. H. Zwietering, I. Jongenburger, F. M. Rombouts, Van ' K., and T. Riet, "Modeling of the Bacterial Growth Curve," Appl. Environ. Microbiol., vol. 56, no. 6, pp. 1875–1881, 1990.